

Spatial and temporal variations in minibasin geometry and evolution in salt tectonic provinces: Lower Congo Basin, offshore Angola

Zhiyuan Ge^{1,2,3}  | Rob L. Gawthorpe³  | Leo Zijerveld³ | Ayodeji P. Oluboyo^{3,4,5}

¹State Key Laboratory of Petroleum Resources and Prospecting, University of Petroleum (Beijing), Beijing, 102249, China

²College of Geosciences, China University of Petroleum (Beijing), Beijing, 102249, China

³Department of Earth Science, University of Bergen, Bergen, Norway

⁴School of Earth, Atmospheric and Environmental Sciences, University of Manchester, Manchester, United Kingdom

⁵PGS, Weybridge, United Kingdom

Correspondence

Zhiyuan Ge, College of Geosciences, China University of Petroleum (Beijing), Beijing, 102249, China.

Email: gezhuyuan@cup.edu.cn; zhiyuan.ge@uib.no

Abstract

In passive margin salt basins, the distinct kinematic domains of thin-skinned extension, translation and contraction exert important controls on minibasin evolution. However, the relationship between various salt minibasin geometries and kinematic domain evolution is not clear. In this study, we use a semi-regional 3D seismic reflection dataset from the Lower Congo Basin, offshore Angola, to investigate the evolution of a network of minibasins and intervening salt walls during thin-skinned, gravity-driven salt flow. Widespread thin-skinned extension occurred during the Cenomanian to Coniacian, accommodated by numerous distributed normal faults that are typically 5–10 km long and spaced 1–4 km across strike within the supra-salt cover. Subsequently, during the Santonian–Paleocene, multiple, 10–25 km long, 5–7 km wide depocentres progressively grew and linked along strike to form elongate minibasins separated by salt walls of comparable lengths. Simultaneous with the development of the minibasins, thin-skinned contractional deformation occurred in the southwestern downslope part of the study area, forming folds and thrusts that are up to 20 km long and have a wavelength of 2–4 km. The elongate minibasins evolved into turtle structures during the Eocene to Oligocene. From the Miocene onwards, contraction of the supra-salt cover caused squeezing and uplift of the salt walls, further confining the minibasin depocentres. We find kinematic domains of extension, translation and contraction control the minibasin initiation and subsequent evolution. However, we also observe variations in minibasin geometries associated with along-strike growth and linkage of depocentres. Neighbouring minibasins may have different subsidence rates and maturity leading to marked variations in their geometry. Additionally, migration of the contractional domain upslope and multiple phases of thin-skinned salt tectonics further complicates the spatial variations in minibasin geometry and evolution. This study suggests that minibasin growth is more variable and complex than existing domain-controlled models would suggest.

This is an open access article under the terms of the Creative Commons Attribution License, which permits use, distribution and reproduction in any medium, provided the original work is properly cited.

© 2020 The Authors. *Basin Research* published by International Association of Sedimentologists and European Association of Geoscientists and Engineers and John Wiley & Sons Ltd.

KEYWORDS

Lower Congo Basin, minibasin, offshore Angola, passive margin, salt tectonics, salt wall, thin-skinned

1 | INTRODUCTION

The dominant tectonic process in passive margin salt basins is gravity-driven, thin-skinned deformation. This is characterized by upslope extension and downslope contraction separated by a domain of translation (e.g. Dooley, Hudec, Pichel, & Jackson, 2018; Fort, Brun, & Chauvel, 2004; Ge, Rosenau, Warsitzka, & Gawthorpe, 2019; Rowan, Peel, & Vendeville, 2004). This configuration develops as a response to regional tilting, resulting from thermal subsidence, tectonic uplift, or basinward differential loading (e.g. Duval, Cramez, & Jackson, 1992; Fort et al., 2004; Hudec & Jackson, 2007; Lundin, 1992; Mauduit, Gaullier, Brun, & Guerin, 1997; Rowan et al., 2004; Vendeville & Jackson, 1992). Previous studies have shown that the upslope migration of the distal contractional domain may result in shifting of the domain boundaries and thus inversion of early extensional salt-related structures (e.g. Fort et al., 2004; Ge, et al., 2019).

Some of the more remarkable morphological features to occur in these kinematic domains are minibasins (e.g. Banham & Mountney, 2013; Gemmer, Beaumont, & Ings, 2005; Hudec, Jackson, & Schultz-Ela, 2009; Jackson & Talbot, 1991; Peel, 2014). These are particularly important because, in contrast with the associated diapirs, they preserve relatively intact record of structural and stratigraphic evolution and hold significant economic resources. The main driving force for minibasin formation has commonly been ascribed to the density contrast between the minibasin fill and underlying salt, where downbuilding of the minibasins is largely driven by sediment deposition which in turn generates more accommodation space for subsequent sedimentation by displacing the underlying salt (Hudec et al., 2009; Jackson & Talbot, 1991). However, data from the Gulf of Mexico suggest that siliciclastic sediments at the time of, or shortly after, deposition are not dense enough to trigger the downbuilding process (Hudec et al., 2009). Along rifted margins as well as other salt basins, alternative triggering forces may include regional tectonics, either extension (e.g. Hodgson, Farnsworth, & Fraser, 1992; Vendeville & Jackson, 1992), or contraction (e.g. Hudec et al., 2009; Ings & Beaumont, 2010), or sediment differential loading (e.g. Goteti, Ings, & Beaumont, 2012; Peel, 2014). Only when the sediments are sufficiently buried and compacted, do they become dense enough for the downbuilding process to occur and to become the main control on minibasin development (Hudec et al., 2009).

Highlights

- We use high quality 3D seismic to document the evolution of a network of minibasins and their associated salt-related structures. We show that minibasin initiation and subsequent evolution can be controlled by different mechanisms and therefore categorising minibasins into simple domain-related types is problematic.
- Variations of minibasin geometry can occur due to along-strike occurrence and linkage of depocentres, which is closely associated with the three-dimensional development of salt-related structures.
- Minibasins at different stages of maturity may also show variations in geometry as neighbouring minibasins can have varying growth rates.
- Upslope migration of contraction can further complicate minibasin geometries as minibasins with different pre-existing geometries respond to the change differently.

In a typical passive margin salt basin, where different kinematic domains interact (e.g. Fort et al., 2004; Marton, Tari, & Lehmann, 2000), multiple controlling factors are expected to contribute to the development and evolution of minibasins (Hudec et al., 2009; Peel, 2014). How minibasins respond to different controls is not well-documented. In particular, the influence of domain changes and multiple phases of salt tectonic deformation on minibasin evolution is poorly understood. Such a lack of knowledge inhibits our analysis of minibasin evolution and can result in an oversimplified categorization of minibasins into those driven by extension, sediment-loading or contraction. The difficulty in carrying out such studies is obvious, as it requires a regional coverage of high-quality seismic data that are large enough to cross multiple kinematic domains.

In this study, semi-regional extensive 3D seismic data covering a c. 4000 km³ portion of the Lower Congo Basin (offshore Angola; Figure 1a) provide an opportunity to document the structural style and tectono-stratigraphic evolution of a network of intraslope minibasins that occur in an area that covers different kinematic domains. Our results show that the tectono-stratigraphic evolution of neighbouring minibasins can vary significantly and that systematic variations in minibasin geometry can provide

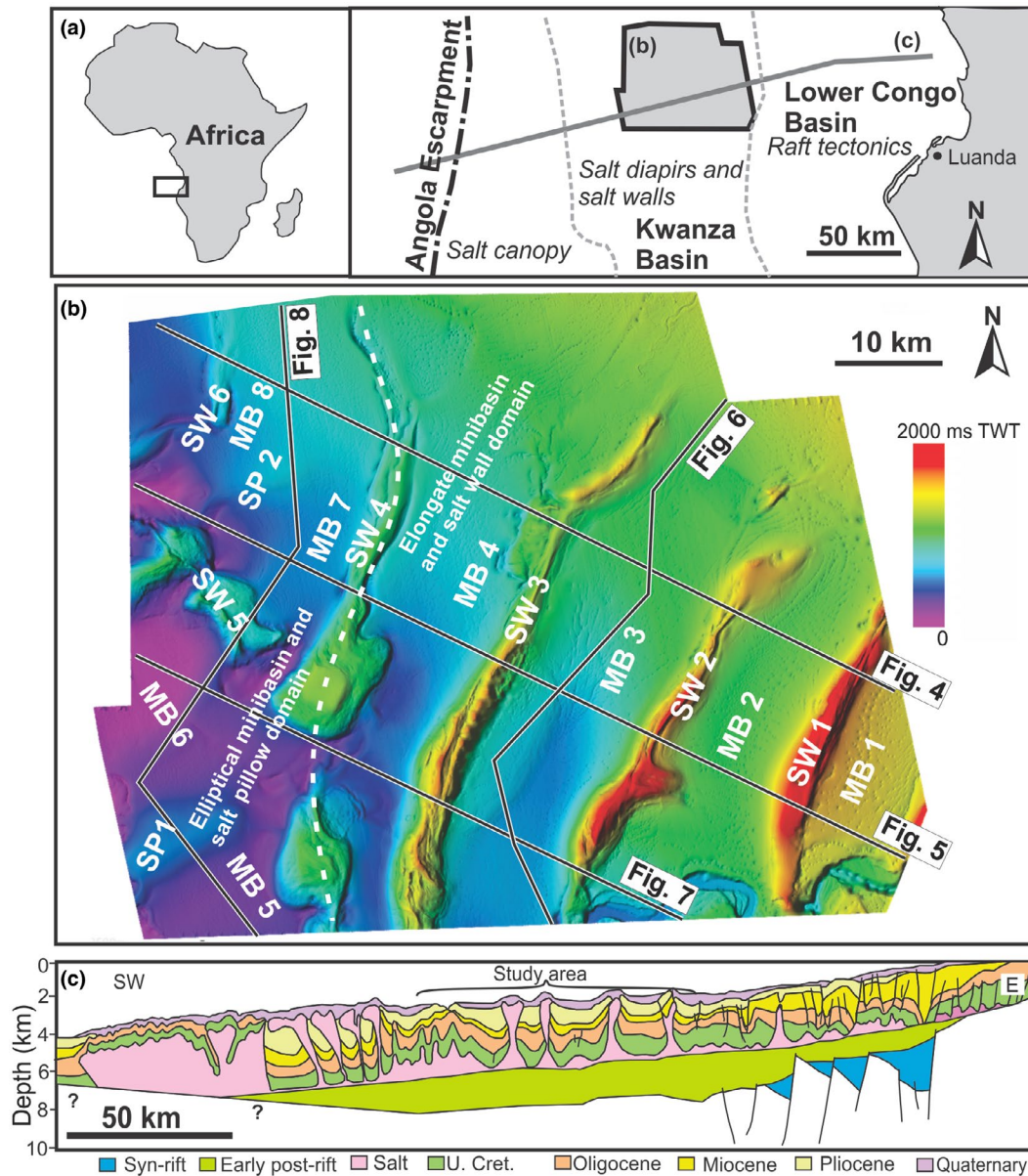


FIGURE 1 (a) Location of the study area. (b) Two-way travel time structure map of the seafloor illustrating the main structural elements in the study area. The dash line marks the boundary between the elongate and elliptical minibasin domains. MB, minibasin; SP, salt pillow; SW, salt wall. (c) Regional seismic profile crossing the Lower Congo Basin (modified after Martonet et al., 2000), showing the 200 km long, thin-skinned gravity-driven system developed above the salt. Approximate location of the study area on this regional profile is indicated

helpful guidelines in understanding the controls on minibasin evolution.

2 | GEOLOGICAL SETTING

The Lower Congo Basin is a 200 km long, N-S-striking salt basin that extends from the coastline of Angola in the east, to the Angola escarpment at the base of Angolan continental slope in the west (Anka, Seranne, Lopez, Scheck-Wenderoth, & Savoye, 2009; Cramez & Jackson, 2000; Marton et al., 2000; Figure 1a). It is one of a series of salt

basins that developed along the west African passive margin associated with the breakup of Gondwana and opening of the Atlantic Ocean (Marton et al., 2000; Moulin et al., 2005; Nürnberg & Müller, 1991). Late Jurassic to Early Cretaceous rifting was followed by the formation of an Aptian sag basin within which approximately 1 km of evaporites accumulated (Loeme Formation; Anderson, Cartwright, Drysdall, & Vivian, 2000; Anka et al., 2009; Brice, Cochran, Pardo, & Edwards, 1982; Karner, Driscoll, McGinnis, Brumbaugh, & Cameron, 1997; Marton et al., 2000; Valle, Gjelberg, & Helland-Hansen, 2001; Figure 2). Following deposition of the Loeme Formation, a shallow-water carbonate-dominated

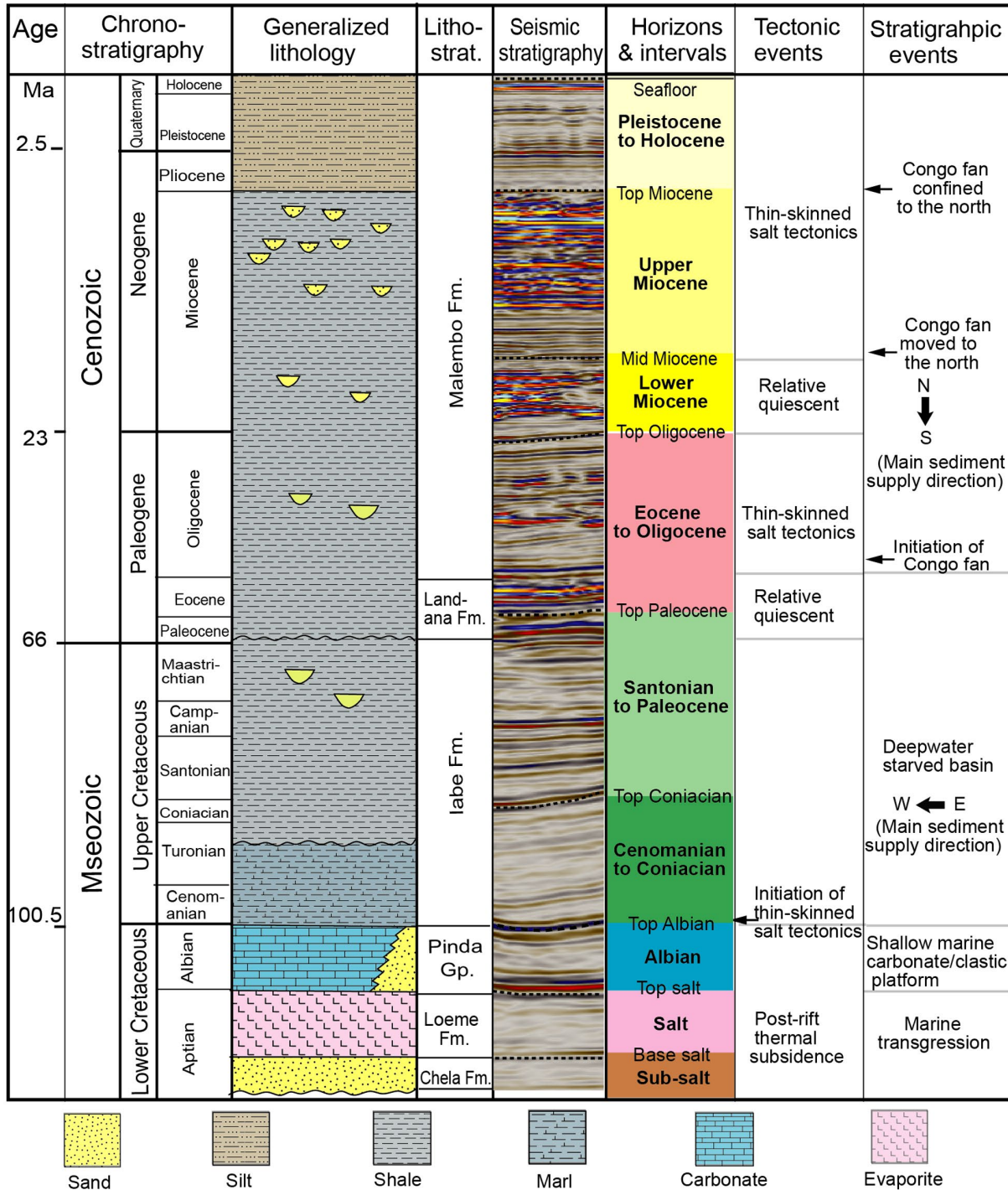


FIGURE 2 Stratigraphy and interpreted horizons of the Lower Congo Basin (modified after Anderson et al., 2000, Valle et al., 2001, Oluboyo et al., 2014 and Ge, Gawthorpe, et al., 2019)

platform developed (Pinda Group) during the Albian (Anderson et al., 2000; Valle et al., 2001; Figure 2). Thin-skinned salt tectonics commenced by the end of the Albian, characterized by the formation of salt-detached normal faults in the upslope area, and contemporaneous folding and thrusting downslope (Fort et al., 2004; Marton et al., 2000; Valle et al., 2001). This shallow marine environment gave way to deep marine conditions during Late Cretaceous, leading

to a transition to the mudstone-dominated Iabe Formation (Anderson et al., 2000; Valle et al., 2001). Deep marine conditions with low sedimentation rates persisted into the Eocene (Landana Formation) until the ancestral Congo River began to supply large volumes of siliciclastic sediments to the Lower Congo Basin from the Oligocene onwards, resulting in an increase in sandy gravity flow deposits in the Malembo Formation (Anderson et al., 2000; Anka & Séranne, 2004;

Valle et al., 2001). Higher sedimentation rates in the upslope area are thought to have enhanced a second phase of thin-skinned extension (Duval et al., 1992; Marton et al., 2000; Valle et al., 2001). Continued shortening and the formation of new contractional structures in distal, downslope areas occurred to accommodate upslope extension, and was associated with the emplacement of the Angola Escarpment (e.g. Anka et al., 2009; Cramez & Jackson, 2000; Fort et al., 2004; Rowan et al., 2004).

In the Miocene, siliciclastic sediments of the deepwater Congo fan were largely trapped in the intraslope minibasins within the Lower Congo Basin, which is accompanied by a third phase of thin-skinned deformation from the late Miocene (Anderson et al., 2000; Anka et al., 2009; Oluboyo, Gawthorpe, Bakke, and Hadler-Jacobsen, 2014). Since the Pliocene, as the main discharge of the Congo river shifted north, the Congo fan shifted to its present-day location, to the north of the study area (Lavier, Steckler, & Brigaud, 2001). Overall, the estimated cumulative movement from three phases of thin-skinned deformation is c. 13 km in the mid-slope area (Marton et al., 2000).

3 | DATASET AND METHODOLOGY

This study utilized part of a proprietary, pre-stack time-migrated 3D seismic survey, covering an area of approximately 4000 km² (Figure 1a). The survey has an inline and crossline spacing of 50 m with a record length of six seconds two-way travel time (TWT). The data quality is generally excellent within the interval of interest (above the salt) but diminishes towards salt walls, often due to steeply dipping beds near the flanks of the salt structures and shielding by overhanging salt. The display of the seismic data follows SEG normal polarity, where a downward increase in acoustic impedance is represented by a peak and is displayed in red. Two wells with conventional well-log suites and proprietary, confidential biostratigraphic reports were used to constrain the age of mapped horizons.

Stratal terminations, and major changes of seismic facies and package thickness were used to define nine regionally continuous and chronostratigraphically significant seismic horizons (Figure 2). The base salt and top salt horizons delineate the salt layer of the Loeme Formation. Mapping these allows us to identify the main salt structures (Figure 3). The base salt horizon is picked at the top of a group of parallel, continuous, moderate to high amplitude reflectors (Figure 2). A severe velocity pull-up affects the base salt horizon under the salt diapirs, and thus the sub-salt structure cannot be precisely constrained (e.g. Figure 4). The top salt horizon is a high amplitude, locally continuous reflector, the continuity of which deteriorates on the steep flanks of salt diapirs (Figure 2).

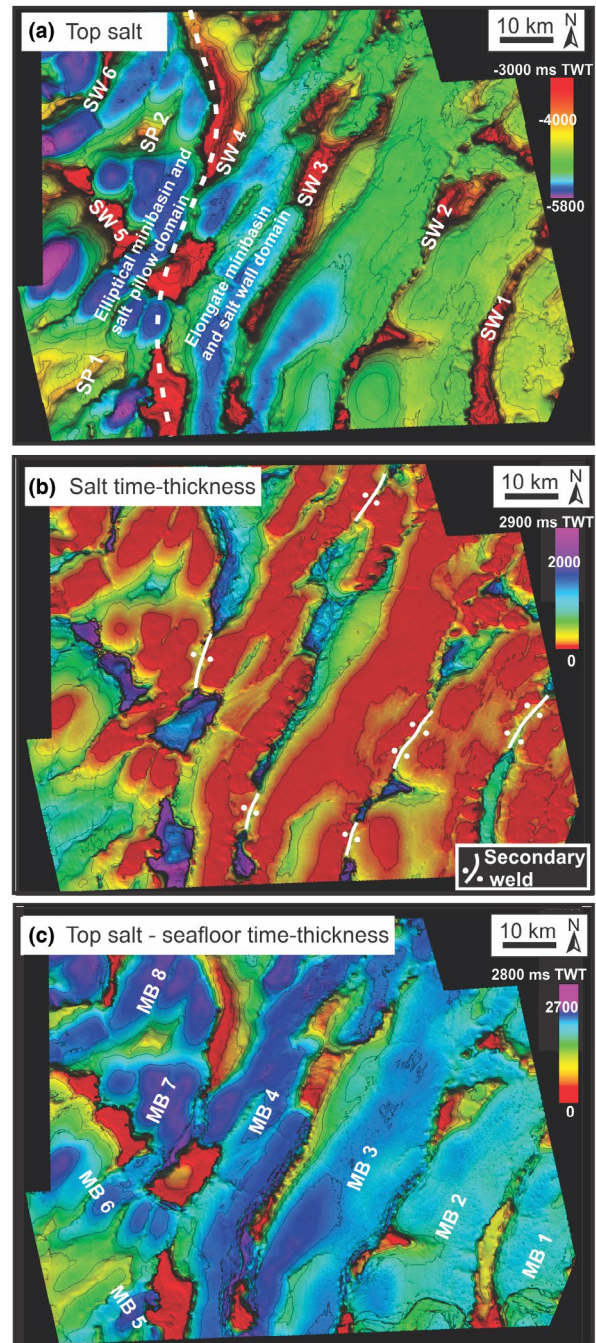


FIGURE 3 Overview maps of the study area. (a) Two-way time (TWT) structure map of the top salt horizon illustrating locations and geometries of the minibasins and salt walls/diapirs, the overall regional slope in the base of post-salt stratigraphy. Note the boundary between the two structural domains. (b) Two-way time thickness of the salt showing the location of salt welds (thin) and salt walls/diapirs (thick). (c) Two-way time thickness from top salt to seafloor showing post-salt deposits and salt-cored highs

Supra-salt cover strata are divided into seven units by six horizons (Figure 2). Among them, the top Albian is a high amplitude, continuous reflector separating Albian carbonates

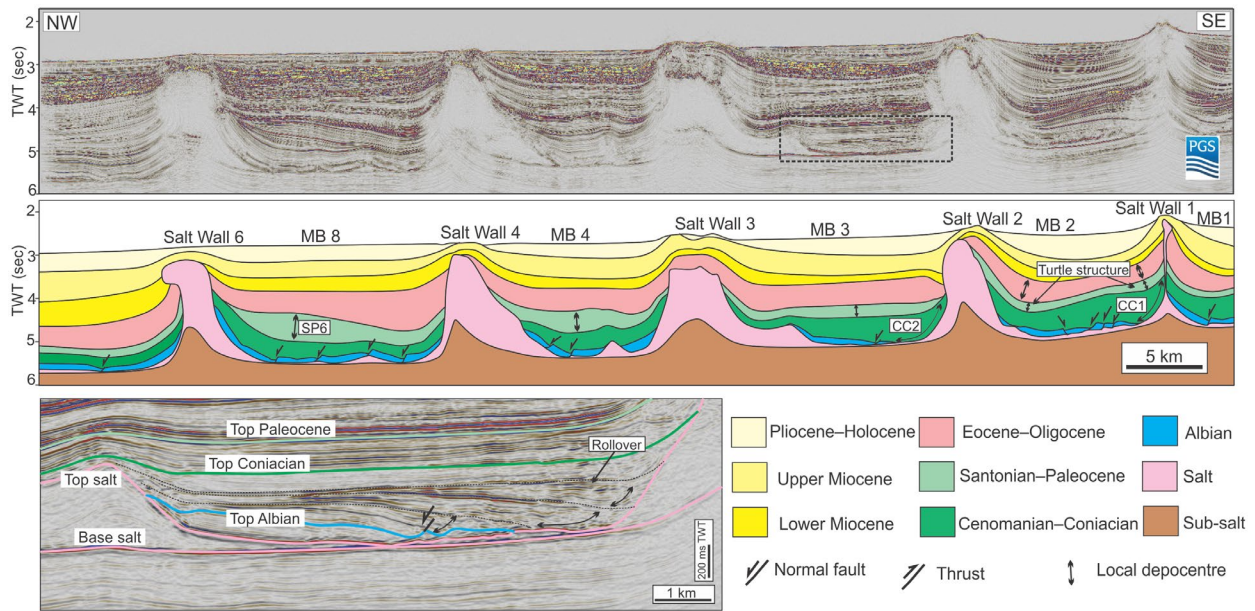


FIGURE 4 Seismic section (above) and interpretation (below) illustrating the structural style of minibasins and salt walls/diapirs in the northeast of the study area. Note the two large rollovers CC1 and CC2 from Cenomanian to Coniacian and severe velocity pull-ups in the sub-salt strata. MB, minibasin. The inset shows details of the rollover CC2. CC1, CC2 and SP6 are described in the text. For location see Figure 3

from the overlying deepwater sediments (Figure 2). The top Coniacian, top Paleocene and top Oligocene horizons usually bound locally thickening strata within minibasins (Figure 2). The mid Miocene and top Miocene horizons follow the scheme of Oluboyo, et al., (2014) subdividing and delineating Miocene turbidite systems (Figure 2).

Two-way travel-time (TWT) structure maps, time-thickness maps and seismic cross-sections were used to describe the structural style and tectono-stratigraphic evolution of the study area. Time-thickness maps were used as a proxy for subsidence and structural activity at the time of deposition. Seismic interpretation was performed in the time domain and therefore geometric distortion, particularly adjacent to salt diapirs and thickness errors around areas of steep dips are to be expected (e.g. Marsh, Imber, Holdsworth, Brockbank, & Ringrose, 2010). We excluded areas of salt overhangs in thickness calculations to avoid over estimation of salt thickness. By cross-checking the observations of map-view variations in time-thickness with cross-sectional stratal geometries, the relationship between salt-related structural activity and post-salt depocentre/minibasin evolution can be confidently discerned. The position of the described structures is always based on their present day locations, although their original locations may be far away from their current locations due to dip-parallel movements that have occurred during thin-skinned extension and contraction (e.g. Marton et al., 2000; their Figure 9). Movement of minibasins and diapirs over base-salt relief may generate local extension and contraction, such as those observed in the Kwanza Basin and the Gulf of Mexico and in modelling studies (Dooley et al., 2018; Duffy

et al., 2019; Evans & Jackson, 2019). However, careful observation suggests no local, linked extension and contraction in the study area and many of the base-salt related topographic features are interpreted as velocity pull-ups located under the salt diapirs. Although we could not explicitly exclude the impact of base-salt relief, the deformation associated with base-salt relief does not play a major role in the study area.

For simplicity and consistence, we refer to all depocentres as minibasins in this study. We do not distinguish between those in contraction (growth synclines or polyharmonic folds; e.g. Fort et al., 2004), and those in extension (rollovers; Hudec et al., 2009). Moreover, we use the term minibasin maturity only to indicate the structural development of a minibasin from subsidence through welding to turtle structure.

4 | PRESENT DAY BASIN GEOMETRY

The study area can be divided into two structural domains based on the tectono-stratigraphic style of the minibasins and salt-cored structural highs, with elongate minibasins and salt walls in the east, and elliptical minibasins and salt pillows in the west (Figures 1a and 3). In both structural domains, salt thickness varies significantly, from apparent, primary salt welds (welding on autochthonous salt), where the thickness of the salt is zero or not resolvable on the seismic (sensu Jackson, Rodriguez, Rotevatn, & Bell, 2014; Wagner & Jackson, 2011) beneath minibasins, to salt diapirs within which salt thickens to more than 2800 ms TWT. Many of

the salt diapirs form topographic highs on the present-day seafloor (Figure 1a).

The elongate minibasin and salt wall domain is characterized by NE-SW-trending minibasins that are >60 km long along strike and extend beyond the study area (Minibasins 1–4; Figure 1a). The minibasins are separated by narrow, curvilinear salt walls of similar length (Salt Walls 1–4; Figure 1a; Figure 3a). The minibasins are mostly welded to the sub-salt strata and are typically 12–20 km wide, with sediment thickness between 2000 and 2800 ms TWT (Figures 3c and 4–6). The bounding salt walls are typically >2000 ms TWT higher than the base of minibasins and range in width from tens of metres, where the salt appears to form secondary welds (welding sub-vertically along salt diapirs; sensu Jackson et al., 2014; Wagner & Jackson, 2011), to 2–5 km (Figures 3b and 4–8). Although these salt walls appear to be continuous on the seafloor (Figure 1a), the salt thickness map indicates significant along-strike variability (Figure 3b). For example, three salt diapirs are found separated by areas where the salt is vertically welded along Salt Wall 4 (Figures 3b and 5). Salt walls may also bifurcate, as seen in the northeastern part of Salt Wall 3 (Figure 3b).

The elliptical minibasin and salt pillow domain is characterized by minibasins that are typically elliptical in shape with the salt-cored structural highs ranging from walls to salt pillows (Figure 3a). The elliptical minibasins (Minibasins 5–8; Figure 3b) are 10–18 km long and of similar width, with sediment thickness between 2000 and 2800 ms TWT. The salt pillows and walls (e.g. Salt Pillow 1 and 2; Salt Wall 5 and 6; Figure 3a) have varied planform geometries

and typically range from 10 to >20 km long and 5 to 10 km wide (Figure 3a). Salt thickness in salt pillows is typically of the order of 1000 ms TWT, shallower than that in salt walls (Figure 3b).

5 | MINIBASIN TECTONO-STRATIGRAPHY

The supra-salt tectono-stratigraphy of the Lower Congo basin shows strong temporal and spatial variations both within and between individual minibasins.

5.1 | Albian

The Albian succession thickens gradually from approximately 100 ms TWT in Minibasin 1, to 150–250 ms TWT in Minibasin 4 and the elliptical minibasin domain to the north-west (Figures 4,5 and 9a). Apparently thick Albian strata (>300 ms TWT) occur around salt-cored structural highs, in particular salt diapirs, are interpreted as artefacts due to the steep dips around these structures (Figures 4 and 9a). Subtle, sub-parallel NE-SW-striking lineations, 5–10 km long and 1 to 4 km apart occur throughout the study area (e.g. Minibasin 4 in Figures 5 and 9a). Thinning of up to 50 ms TWT across these lineaments is thought to be due to a network of normal faults active in the overlying Cenomanian–Coniacian interval.

The absence of large-scale thickness variations and a lack of syn-tectonic growth strata within the Albian succession

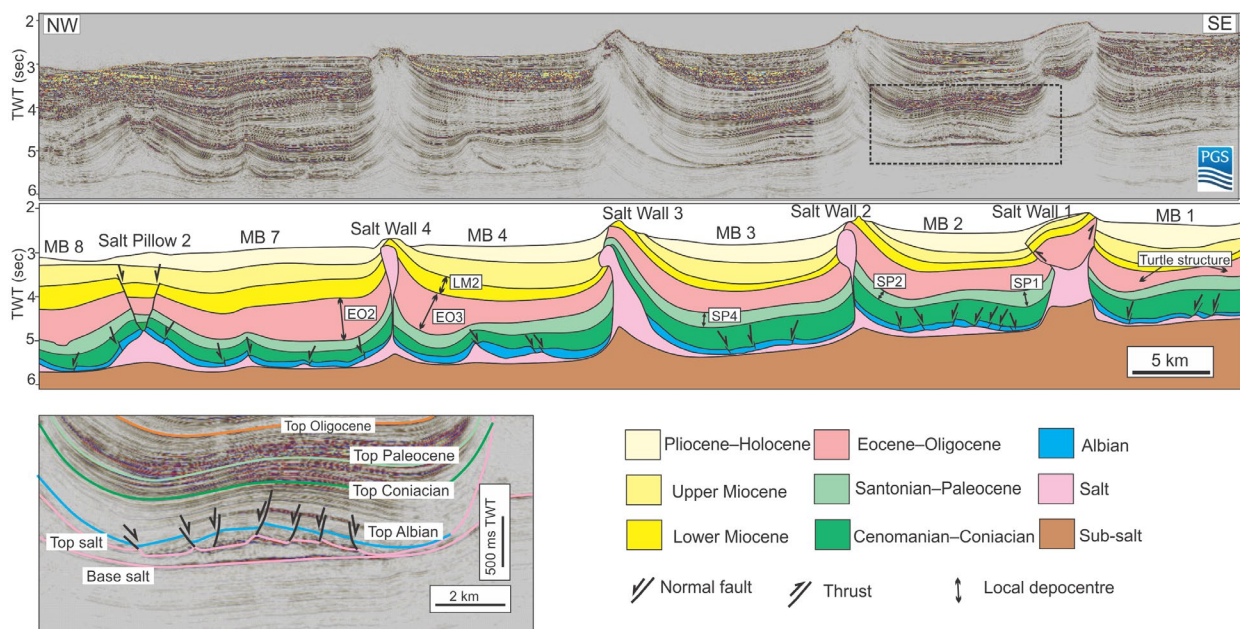


FIGURE 5 Seismic section (above) and interpretation (below) illustrating the structural style of minibasins and salt walls/diapirs in the middle of the study area. MB, minibasin. The inset shows the style of Cenomanian to Coniacian normal faults. SP1, SP2, SP4, EO2, EO3 and LM2 are described in the text. For location see Figure 3

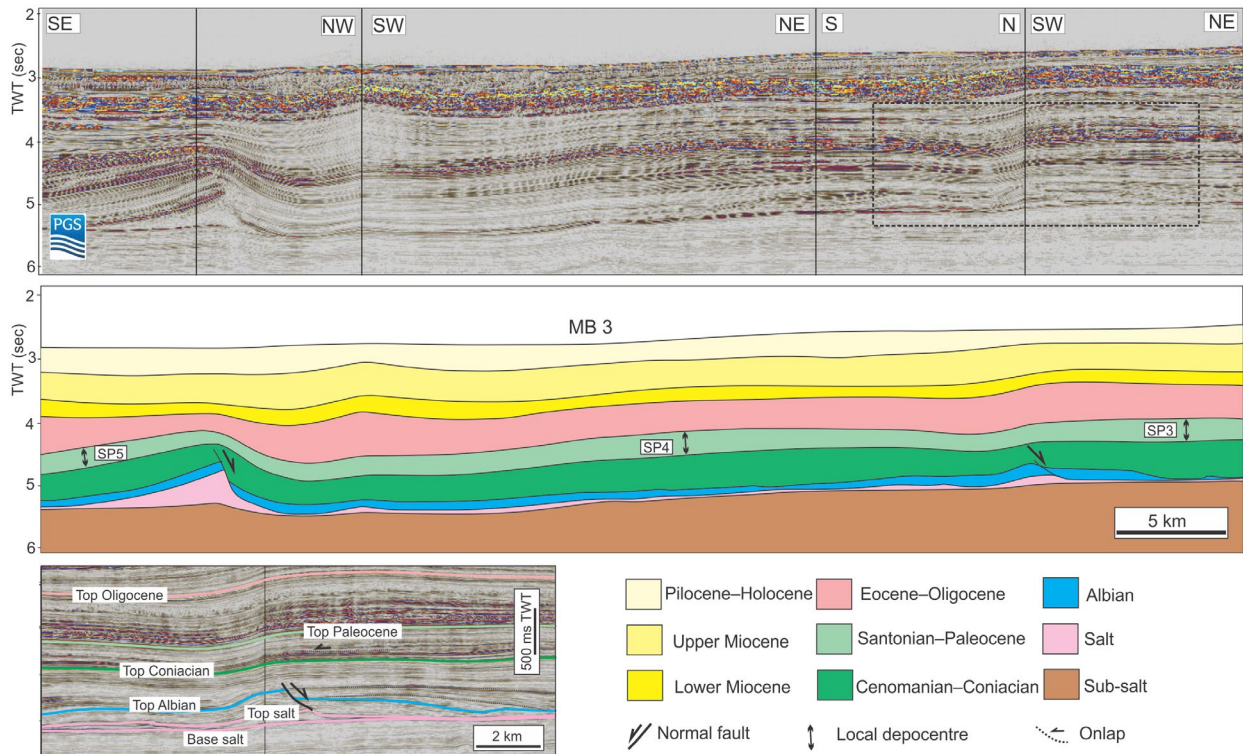


FIGURE 6 Seismic section (above) and interpretation (below) illustrating the along-strike structural style of Minibasin 3. Note the two salt rollers define the boundaries between SP3, SP4 and SP5. MB, minibasin. The inset shows details of a salt roller. Note the onlaps against the salt roller. SP3, SP4 and SP5 are described in the text. For location see Figure 3

are in agreement with previous work in the area that interprets the Albian as pre-kinematic with regards to the main phase of salt-tectonic activity (e.g. Fort et al., 2004; Valle et al., 2001).

5.2 | Cenomanian–coniacian

The overall thickness of the Cenomanian–Coniacian succession decreases from 800 ms TWT in the east of the study area to 200–300 ms TWT in Minibasin 4 and further west (Figures 5 and 9b). To the northeast of Minibasin 2 and 3, two listric normal faults sole out northwestwards into the salt, developing rollovers with a thickened succession, up to 800 ms TWT thick, in their hanging walls (CC1 and CC2; Figures 4 and 9b). A network of NE–SW-striking normal faults is developed across the study area with local thick stratigraphy in small hanging wall depocentres (Figures 4–6). These normal faults correspond to the linear features observed in the Albian strata. Typically, the faults dip to the northwest, are 5–10 km long, have a spacing of 1 to 4 km, and a maximum throw of 120 ms TWT (Figure 9b). In cross-section, the faults rarely offset the top Coniacian (Figures 4–6).

The abundance of NE–SW-striking normal faults suggests that the study area underwent NW–SE thin-skinned extension above the salt during the Cenomanian to Coniacian. The timing of initial extension corresponds to onset of the development

of extensional raft tectonics further upslope, to the east of the study area (Duval et al., 1992; Marton et al., 2000; Valle et al., 2001; Figure 1b). However, normal faulting ceased in the study area by end Coniacian given that no faults extend into the overlying, younger, strata (Figures 4a and 8b). Such fault deactivation occurred earlier than what has been observed in the upslope raft domain, where the first phase of extension continued into the Santonian and later times (Valle et al., 2001). Such differences probably relate to the upslope retreat of the extensional domain, which has been observed in analogue modelling studies of passive margin salt tectonics (Fort et al., 2004; Ge, et al., 2019).

5.3 | Santonian–paleocene

The Santonian–Paleocene succession shows significant local thickness variations, between 240–700 ms TWT, across the study area (Figures 4 and 9c). In the elongate minibasin domain, two depocentres (SP1 and 2; Figure 9c), 3 km wide by 10 km long, and containing 250–300 ms TWT of Santonian–Paleocene strata, developed on the flanks of Minibasin 2, adjacent to Salt Wall 1 and 2 (Figure 9c). This depocentre geometry represents a typical turtle structure where the succession thickens from middle to the flanks of the minibasin. In contrast, three 10–20 km long and up to 6 km wide depocentres (SP3, 4 and 5; Figure 9c) lie broadly along the

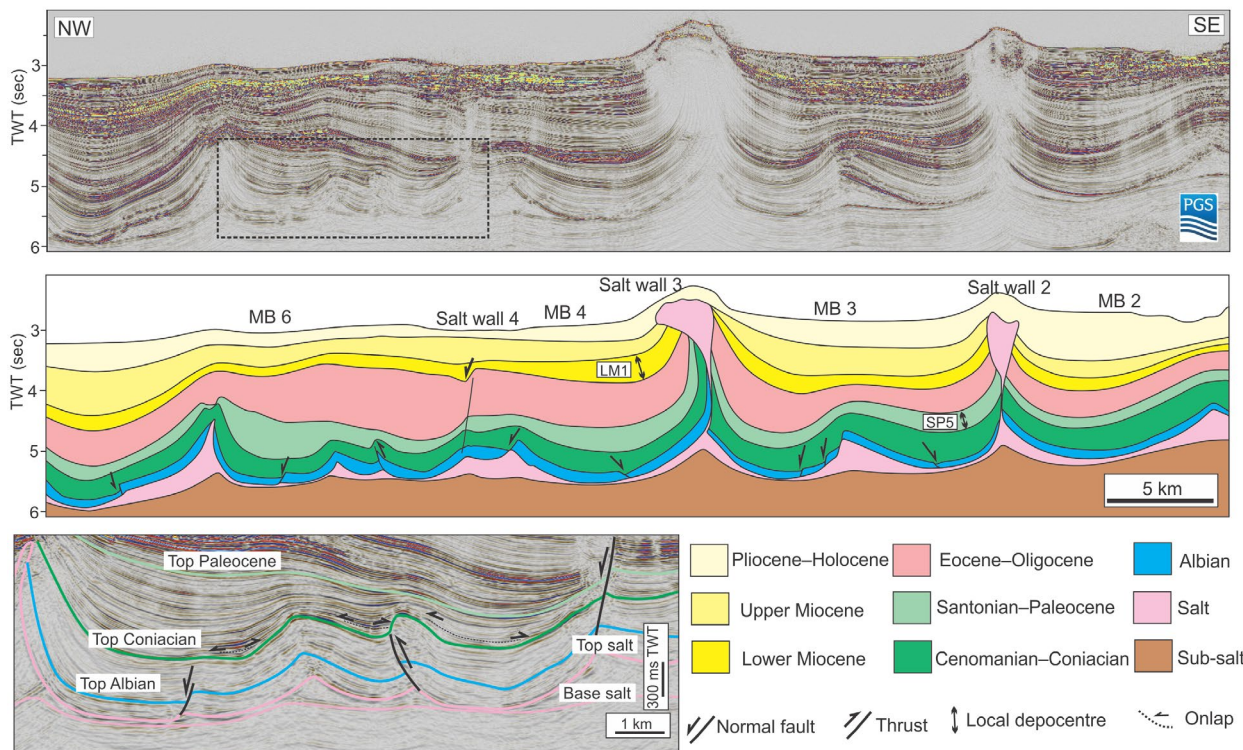


FIGURE 7 Seismic section (above) and interpretation (below) illustrating the structural style of minibasins and salt walls/diapirs in the south of the study area. Note the thrusts and folds from Santonian to Paleocene. MB, minibasin. The inset shows details of the thrust and fold geometry. SP5 and LM1 are described in the text. For location see Figure 3

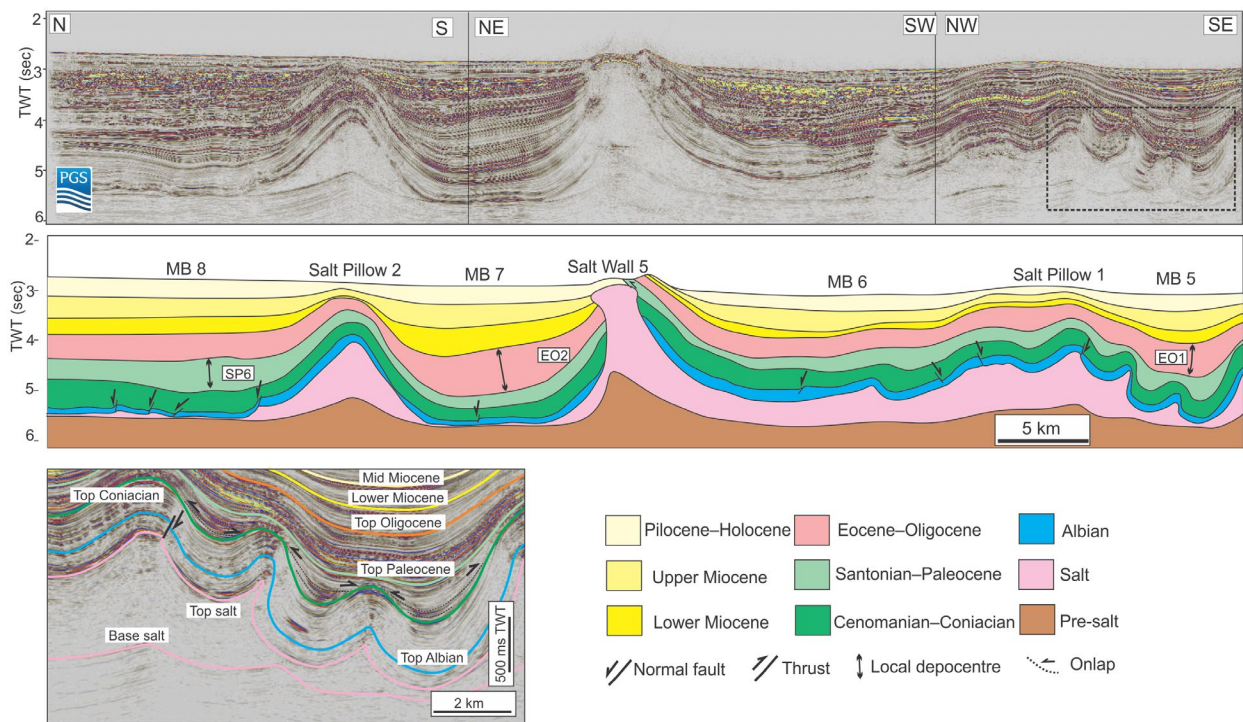


FIGURE 8 Seismic section (above) and interpretation (below) illustrating the structural style of minibasins and salt pillows and diapirs in the west of the study area. MB, minibasin. The inset shows the details of the folds developed from Santonian to Paleocene. EO1, EO2 and SP6 are described in the text

strike of Minibasin 3, and contain up to 360 ms TWT of strata that in cross-section are bowl-shaped and thin onto flanking

salt walls (Figure 9c). The along-strike section shows that these depocentres are laterally continuous but with the strata

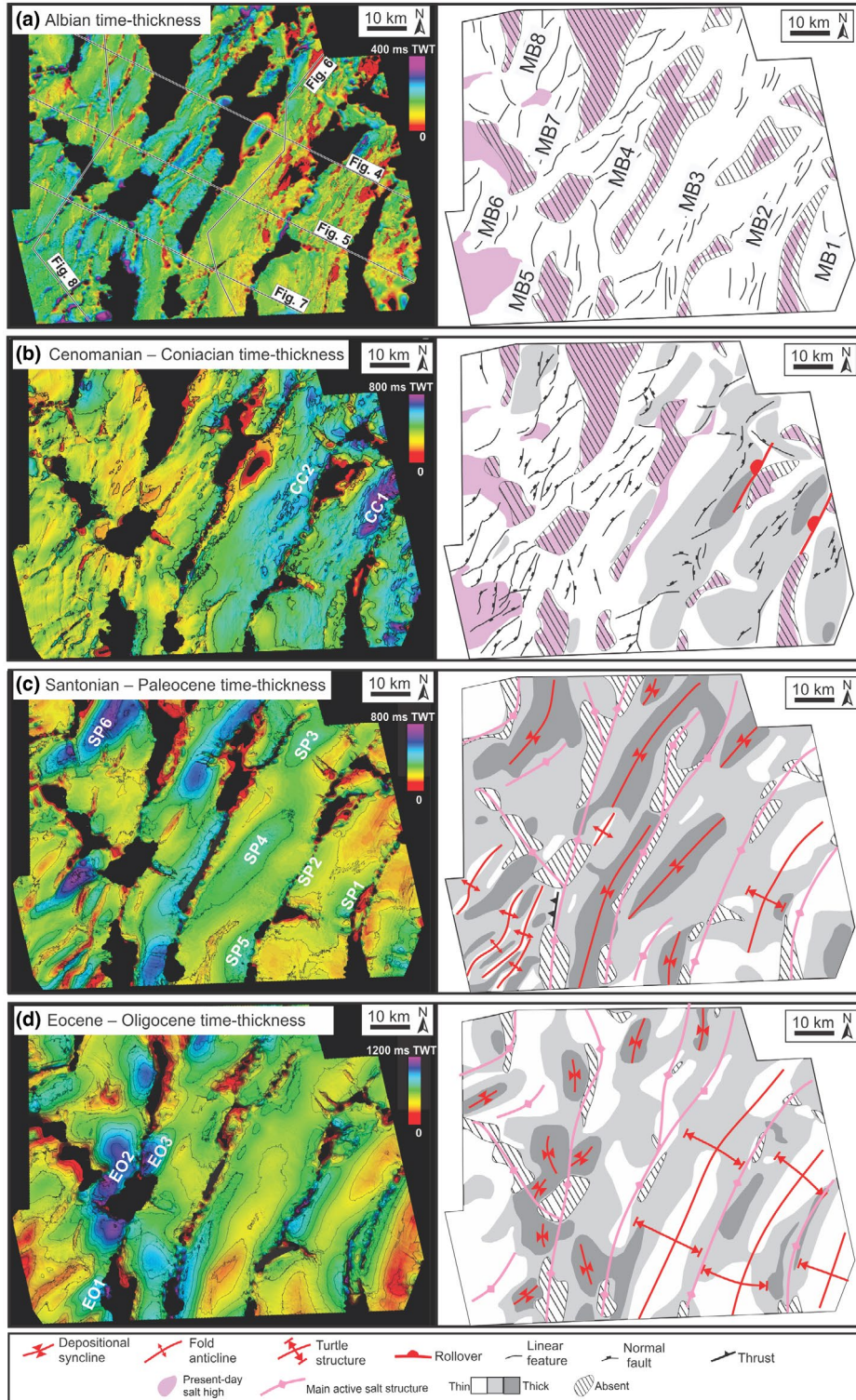


FIGURE 9 Two-way time thickness maps (left) and interpreted structural/topographic features for the seven supra-salt stratigraphic intervals (right). (a) Albian time-thickness map, linear features indicate subtle thickness variations due to cut outs along faults that occurred later. (b) Cenomanian–Coniacian time-thickness map with widespread normal faults and the location of two rollover structures CC1 and CC2 observed in the east of MB2 and MB3. Note that this package thins from SE to NW. (c) Santonian–Paleocene time-thickness map illustrates depocentre distribution and fold and thrust structures. Depocentres SP1–6 are marked on the thickness map. (d) Eocene–Oligocene time-thickness map displays the development of turtle structures in the elongate minibasin domain and distributed depocentres in the elliptical minibasin domain. Depocentres EO1–3 are marked on the thickness map. (e) Lower Miocene time-thickness map displays various depocentres in the study area. Note most depocentres, apart from the depocentre LM1, in the elongate minibasin domain are located along the west of individual minibasins. (f) Upper Miocene time-thickness map illustrates the development of laterally continuous and symmetric depocentres. Depocentres UM1 and UM2 are marked on the left. (g) Pliocene–Holocene time-thickness map shows the development of asymmetrical depocentres and salt-cored folds

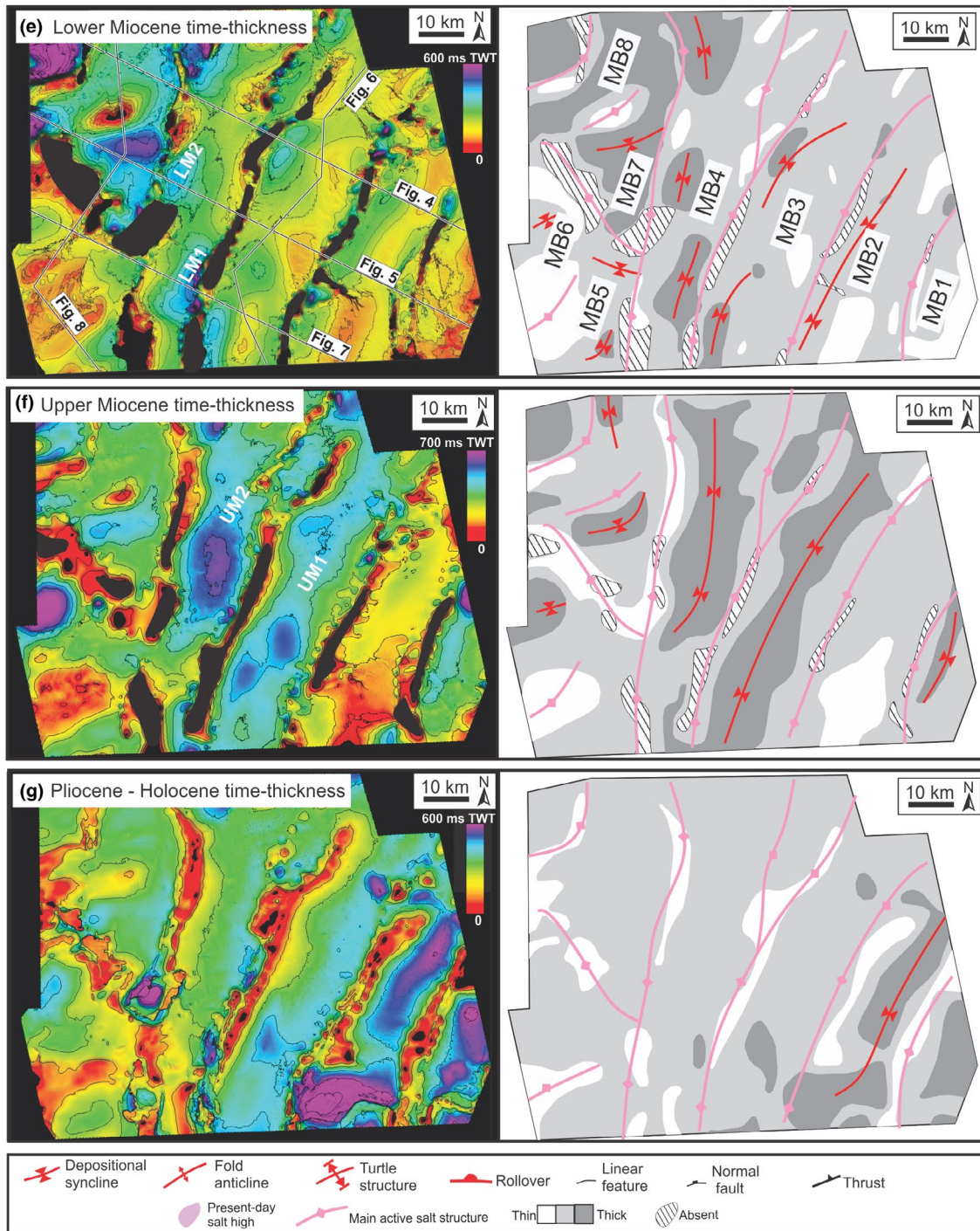


FIGURE 9 (Continued)

thinning over underlying salt rollers associated with previous extension (Figure 6). Depocentres in Minibasin 4 are similar in character.

The depocentres in the elliptical minibasin domain have very different geometries to minibasins in the east. For example, Minibasin 5 and 6, in the southwest of the study area contain several depocentres that are up to 20 km long, 2–4 km wide, and have 300–600 ms TWT of strata within them (Figure 9c). In cross-section, these depocentres contain

growth strata associated with NE-SW-striking elongate folds and thrusts that have a wavelength of 2–4 km (Figures 7 and 8). In contrast, depocentre SP6 occurs broadly in the middle of Minibasin 8 and is >650 ms TWT thick, with strata thinning towards flanking Salt Walls 4 and 6 (Figure 4).

In the Santonian–Paleocene, minibasin development in the elongate and the elliptical minibasin domains was highly variable. The formation of a turtle structure in Minibasin 2 in the elongate minibasin domain suggests that this

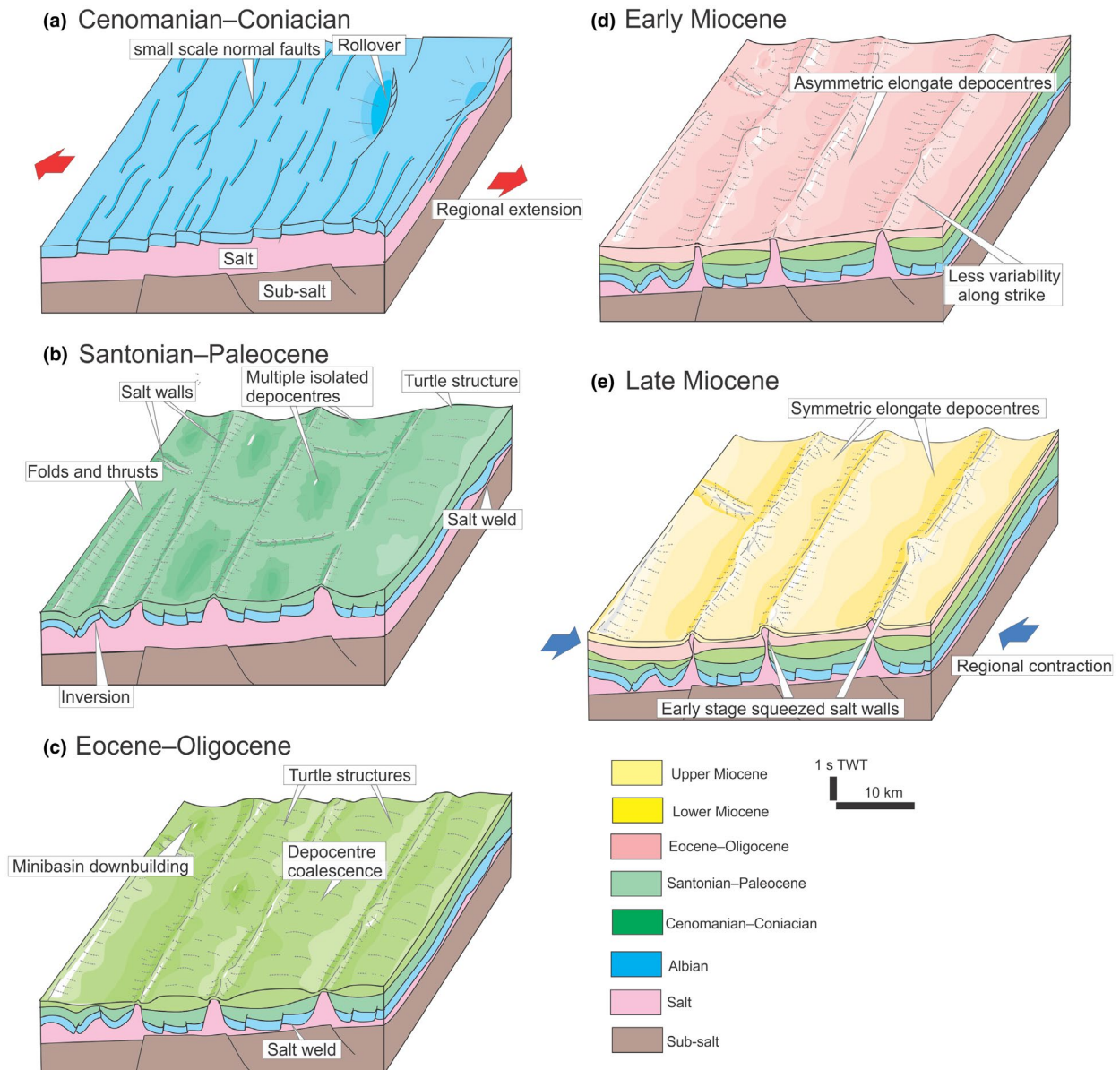


FIGURE 10 Block diagrams illustrating the development of minibasins and associated salt walls in the study area. (a) Cenomanian to Coniacian with widely distributed normal faults and two large rollovers. (b) Santonian to Paleocene with multiple depocentres and turtle structures highlighting different degrees of minibasin maturity. (c) Eocene to Oligocene documented the change from isolated depocentres to elongate minibasins with turtle structures. (d) Early Miocene with depocentres preferentially along the western sides of the minibasins. (e) Late Miocene with squeezed and uplifted salt walls/diapirs

minibasin (c. 1000 ms TWT thick) became welded in the centre halting further subsidence and shifting the locus of subsidence and sediment accumulation deposition towards its flanks (Figure 5). In contrast, the bowl-shaped strata in the Minibasin 3 suggest that salt was still being expelled from beneath the minibasin into adjacent salt walls. The geometry of both these types of minibasins indicates that the main control on subsidence was sedimentary loading (Hudec et al., 2009; Peel, 2014; Rowan & Weimer, 1998), changing from the extension during Cenomanian to Coniacian interval. Similarly, the salt diapirism between the minibasins is interpreted to change from an early reactive phase to a

passive phase. Moreover, the simultaneous observation of bowl-shaped fills and turtle structures in minibasins indicates different stages of minibasin maturity. Such variation is probably related to thicker Cenomanian to Coniacian strata in Minibasin 2 compared with Minibasin 3 that resulted in thinner salt under Minibasin 2. Our observations also suggest that the present-day elongate minibasins initiated as a series of individual depocentres with limited connectivity, during the Santonian which grew and linked subsequently (Figures 6,9c and 10). The linkage areas were generally associated with zones where remnant salt was trapped beneath the minibasin (Figures 3b and 6).

In the elliptical minibasin domain, the narrow, elongate folds and thrusts in Minibasin 5 and 6 suggest that the area experienced thin-skinned contraction during the Santonian to Paleocene. The NE-SW-striking thrust faults and folds in this area are interpreted to result from contraction that had migrated up-dip (Figures 1b,7 and 8). This interpretation of up-dip migration of the contraction domain is consistent with previous studies of the evolution of the contraction domain in the Lower Congo Basin where early formed extensional structures were inverted by late contraction (e.g. Fort et al., 2004). The contraction is thought to end by the Paleocene as no corresponding extension was found in the upslope and the margin overall became tectonically quiescent (Valle et al., 2001).

5.4 | Eocene–oligocene

Most of the Eocene–Oligocene depocentres lie directly adjacent to the flanks of salt-cored structural highs (Figure 9d). In the elongate minibasin domain, depocentres in Minibasin 1–3 are between 700 and 900 ms TWT thick, 3–4 km wide, up to 28 km long, and run along both sides of the minibasins (Figure 9d). In cross-section, these minibasins have the shape of a turtle structure, with relatively thin strata in the centre of the minibasins and thicker strata towards their flanks (Figures 4 and 5). In contrast, in Minibasin 4 and the elliptical minibasin domain, the depocentres have ovate planview geometries and are 5–8 km long and wide, and occur broadly in the middle the minibasins (e.g. EO1 and EO2; Figure 9d), or asymmetrically flanking the salt structures (EO3; Figure 9d). For example, in Minibasin 5 and 6, depocentres EO1 and EO2 have bowl-shape strata which are thickest in the middle of the minibasin and converge towards the salt pillows and salt walls (Figure 8).

In the Eocene to Oligocene succession, the occurrence of turtle structures and the lack of extensional and contractional structures suggests that sediment loading was the dominant mechanism driving minibasin growth. Despite no evidence of extension or contraction in the study area during Eocene to Oligocene, a second phase of extension from late Eocene to late Oligocene occurred in the upslope area of the Lower Congo Basin (Valle et al., 2001). Therefore, we interpret the intraslope minibasins in the study area to be located in a translational domain during this interval.

The Eocene to Oligocene minibasins show a range of structural styles that we interpret to reflect different stages of maturity. Over most of the elongate minibasin domain (Minibasin 1–3), turtle structures suggest that the minibasins were mature and largely welded along the basin axes. In contrast, the depocentres with bowl-shaped geometry in the elliptical minibasin domain and Minibasin 4 indicate that these minibasins still had mobile salt beneath them allowing

continued subsidence and expulsion of salt into adjacent salt walls or pillows (Figure 8). We interpret these variations in minibasin maturity as a result of higher sediment supply in the east of the study area compared to the west on the basis of thickness variations. For example, the Albian–Paleocene strata are over 1000 ms TWT in Minibasin 1–3 but reduce gradually to c. 600 ms TWT in Minibasin 7 (e.g. Figure 5).

5.5 | Lower miocene

The Lower Miocene succession shows overall thickening from approximately 100 ms TWT in the southeast of the study area, thickening to more than 500 ms TWT in the northwest (Figure 9e). In the elongate minibasin domain, strata in Minibasins 1–3 thicken towards the western flank of the minibasins, reaching 300–350 ms TWT in thick areas. In cross-section, the depocentres are asymmetric and westward thickening up to 6 km wide and 8–18 km long (Figures 4–8). In contrast, the depocentres in Minibasin 4 distribute in both sides of the minibasin. For example, a 15 km long and 8 km wide depocentre, LM1, with over 350 ms TWT of Lower Miocene strata, occurs along the eastern flank of Minibasin 4, and a nearby depocentre, LM2, is located along the northwestern flank of the minibasin (Figures 7 and 9e). Depocentres in the elliptical minibasin domain contain > 500 ms TWT of strata and thin onto flanking salt-cored structural highs (Figure 9e). Notably, we observe some extensional deformation in this interval: a normal fault above Salt Wall 4 (Figure 7) and a small crestal graben above Salt Pillow 2 (Figure 5).

The geometry and distribution of the Lower Miocene succession is interpreted to be controlled by a combination of regional tilting and variations in sedimentation. A plausible explanation for the asymmetrical stratal thickening towards the flanking salt-cored structures is regional contraction. Although the crestal graben can also be explained by outer-arc extension associated with regional contraction, such explanation seems at odds with the extensional fault we observe above Salt Wall 4. Furthermore, a previous study has also suggested a third phase of thin-skinned contraction started in the late Miocene (Valle et al., 2001). We therefore interpret the preferential distribution of depocentres in Minibasins 1–3 in the west as a result of northwest tilting of the margin associated with the uplift of the African continent (Anka & Séranne, 2004; Lavier et al., 2001). We speculate that tilting caused the northwestern parts of the minibasins to become relative topographic lows focusing sediment transport and accumulation in those areas. An alternative interpretation is that tilting is local and associated with migration over base-salt topography, such as those observed in the Kwanza Basin (Evans & Jackson, 2019). Sediment loading still was an important control in the elliptical minibasin domain, with

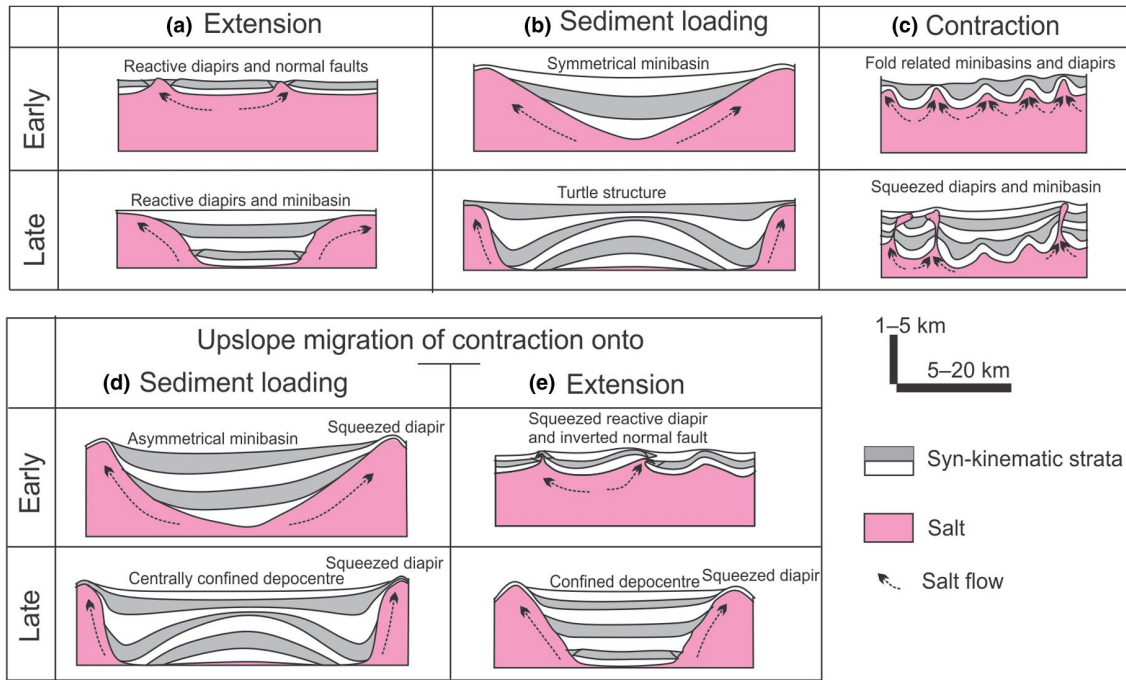


FIGURE 11 Minibasin geometry and stratigraphy under various driving mechanism, maturity and upslope migration of the contractional domain. Note the scale is tentative to reflect the vertical exaggeration. (a) Minibasin development controlled by extension. Note the extension is partially accommodated by diapir as cryptic extension (early and late). (b) Minibasin development controlled by sediment loading. Note the early symmetrical minibasin (early) and more mature turtle structure (late). (c) Minibasin development associated with contraction as early fold- and thrust-related minibasins (early) are modified by breach of salt into diapirs (late). (d) Main control of minibasin evolution changes from sediment loading to contraction. Note the different geometries as the change occurs in early and late stages during minibasin downbuilding. (e) Main control of minibasin evolution changes from extension to contraction. Note the different geometries of minibasins as the inversion occurs in early versus late during extension. See the text for discussion and reference

continued salt withdrawal and depocentre subsidence surrounding Salt Pillow 2 and the southern end of Salt Wall 4.

5.6 | Upper miocene

The Upper Miocene has very variable sediment thicknesses both between and within minibasins. For example, depocentres in the Minibasin 3 and 4 are up to 50 km long and 15 km wide, and are locally > 600 ms TWT thick (Figure 9f). These thick accumulations contrast with Minibasin 2, 6 and 7 with in which the strata are *c.* 200 ms TWT thick (Figure 9f). In contrast with the Lower Miocene, where depocentres usually lie on the flanks of salt-cored structural highs, Upper Miocene depocentres are located along the centre of the Minibasins 3, 4 and 5 (Figure 9f). In cross-section, the Upper Miocene strata always thin towards the bounding salt-cored structural highs forming growth wedges (Figures 4 and 5).

The Miocene, as a whole, is a period of relatively high sediment supply as evidenced by the widespread occurrence of sandy turbidite channels and lobes (e.g. Oluboyo et al., 2014). Some of the thickness variations observed between minibasins, particularly in the Upper Miocene interval, were due to the sediment routing being fixed to particular

minibasins (e.g. Minibasin 3), whereas others were relatively sediment starved (e.g. Minibasin 2). During the late Miocene, all the minibasins were welded in the study area (Figure 9e). Thinning of strata towards the salt diapirs, however, suggests that sediment accumulation occurred along the basin centres, which is interpreted to be a result of the rise of the salt-cored structures. The growth and elevation of salt diapirs is interpreted to result from thin-skinned contraction that squeezed the weak, salt-cored structures (active diapirs Calot et al., 2012; Rowan & Vendeville, 2006). This contraction affected the entire study area and coincided with a third phase of upslope extension to the east of the study area (Valle et al., 2001).

5.7 | Pliocene–holocene

The Pliocene–Holocene succession gradually thins from approximately 700 ms TWT in Minibasin 1 and 2 in the elongate minibasin domain, to just over 300 ms TWT in the elliptical minibasin domain (Figure 9g). Overall, the depocentres form elongate wedges along the centre of the minibasins that thin onto the flanking salt-cored highs (Figure 4). Many of the growth wedges are asymmetrical, with the thickest strata

present along their eastern sides (e.g. Minibasins 3 and 4; Figure 4). These asymmetrical growth wedges are associated with thrusts and vertical salt welds where the eastern limb of the salt wall is welded and/or thrust over its western limb (e.g. Salt Wall 2; Figure 5).

The Pliocene–Holocene succession is similar to the late Miocene with growth strata confined by the growing salt-cored structural highs (Figure 4). However, the sedimentary system shows clear evidence of rerouting. For example, the Minibasin 2 has the thickest strata of the Pliocene–Holocene interval, whereas it was sediment starved during the late Miocene (Figure 8g). More importantly, in contrast with the late Miocene, where depocentres developed along the axis of the minibasins, the Pliocene–Holocene growth wedges were asymmetrical and focused along one side of the minibasin. Such asymmetry is related to thrusting and contraction continued from late Miocene (Figure 5; Valle et al., 2001).

6 | DISCUSSION

Mapping of key stratigraphic surfaces and analysis of time-thickness maps and cross-sectional stratal geometries show that the location and geometry of minibasins, and flanking salt-cored highs, varied in time and space. We propose that such variability is controlled by a number of interacting mechanisms that vary in space and time. In this section, we discuss the 3D development of the minibasins, the spatial and temporal variability of minibasin geometry and how these are influenced by minibasin maturity as well as the impact of kinematic domain migration.

6.1 | Three-dimensional development of minibasins

Previous studies of passive margin salt basins have generally considered minibasin development in conjunction with salt-related structures along the dip-orientated transects from the basin margin to the toe of slope (Brun & Fort, 2012; Duval et al., 1992; Ings & Beaumont, 2010; Mauduit et al., 1997; Peel, 2014; Rowan et al., 2004). For example, in a benchmark paper on minibasin formation, Hudec et al. (2009) summarize the geometric and stratigraphic character of minibasins under sedimentary loading, contraction and extension in 2D. Extension creates reactive diapirs where salt may rise into rollers, and rollover anticlines in the hanging wall of thin-skinned listric normal faults (e.g. Figure 4; e.g. Gemmer et al., 2005; Mauduit et al., 1997). Minibasins driven by sediment loading typically have a bowl-shaped geometry with a central topographic low and relatively thick syn-tectonic strata that thin onto the surrounding salt-cored highs (Figure 4; e.g. Hudec et al., 2009; Peel, 2014). In contrast,

contraction may form salt-detached folds and thrusts, the former being cored by salt pillows (Figures 5 and 10e; Brun & Fort, 2004; Hudec et al., 2009). Such contractional minibasins are sometimes referred as polyharmonic folds as they continue to grow under contraction (Fort et al., 2004).

Our analysis of 3D seismic data from the Angola margin also shows strong along-strike variability in minibasin development. The present-day configuration of elongate minibasins started off from a pervasive network of small-scale normal faults (Figure 10a) and a few large rollovers in the hanging wall of rare large normal faults (e.g. CC1 and CC2 in Figure 9b). Later, a number of distinct depocentres, up to 20 km long, developed which subsequently grew and merged into single, elongate minibasins (>50 km long). For example, during the Santonian to Paleocene, three depocentres (SE3–5), separated by underlying salt rollers, occurred along what is now Minibasin 3. During the Eocene to Paleocene, these three depocentres merged into a single minibasin that was largely welded on sub-salt strata and the influence of the salt roller became negligible (Figures 6 and 10b,c). From the Miocene onwards minibasins showed less along-strike variability (Figure 10d and e) as regional tilting and subsequent thin-skinned contraction took control. Although an explicit, more detailed analysis of the along-strike evolution of minibasins is beyond the scope of this study, our results suggest that the along-strike growth and heterogeneity in large, elongate minibasins is closely related to the three-dimensional development of salt-related structures, such as salt rollers (Figure 6). As they grow and rise, they separate the depocentres occurring above them. However, once they cease to grow, either due to the cut-off of salt supply or the change of regional tectonics, depocentres gradually coalesce into larger minibasins.

6.2 | Variability of controlling mechanism and minibasin maturity on minibasin evolution

The growth of minibasins on passive margins is interpreted to result from a range of different driving mechanisms that generate characteristic stacking patterns within associated syn-growth strata (e.g. Brun & Fort, 2011; Hudec et al., 2009; Peel, 2014; Figure 10). As a result, changes in the mechanisms driving minibasin formation and evolution can result in marked variability in minibasin geometry and growth strata architecture.

The results of this study, in addition to documenting lateral growth and depocentre coalescence during minibasin development, highlights the variability in minibasin geometry during their evolution. As a minibasin matures, it eventually welds onto underlying sub-salt strata. Because minibasins develop at different rates, minibasins at different stages of

maturity can co-exist, particularly during the early stages of minibasin evolution (Figure 11a–c). In minibasins dominated by sediment loading (downbuilding; Figure 11b), the underlying salt eventually depletes and the supra-salt strata weld onto the sub-salt strata below. During the welding process, the stacking geometry of the minibasin strata changes from a bowl-shaped to a turtle geometry, in which the depocentres migrate to the flanks of the minibasin (Figure 11c). An example of typical minibasin downbuilding geometry with a central bowl-shaped strata can be seen in the Santonian to Paleocene interval in Minibasin 3, while only a few kilometres away to the east across Salt Wall 2, Minibasin 2 had already developed a central turtle structure (Figures 4 and 9c). Furthermore, these different minibasin geometries responded differently to changes in the mechanism driving minibasin geometry. In the southwestern part of the study area, contraction occurred during the Santonian when the extensional minibasins were in their early stages of development, which resulted in small wavelength, elongate folds and related thrusts due to the relatively thin cover strata (Figure 8). In contrast, the late Miocene contraction, when the minibasins were more matured and welded, and consequently relatively strong, resulted in squeezing of pre-existing diapirs (Figure 11b).

Based on the examples gathered from this study and those published from other studies and other passive margin salt basins, we recognize six typical minibasin geometries controlled by various driving mechanism and maturity (Figure 11). Typically, gravity driven thin-skinned salt tectonics have kinematic domains of extension, translation and contraction (e.g. Fort et al., 2004; Rowan et al., 2004). Correspondingly, the main minibasin controls of extension, sediment loading and contraction, are generally associated with these three kinematic domains (Figure 11a–c). In the extensional domain, minibasins may occur with extensional diapirs and normal faults followed by welding on the sub-salt with extension accommodated by diapirs (cryptic extension; Figure 11a; e.g. Jackson, Vendeville, & Schultz-Ela, 1994). In the translation domain, sediment loading forms early symmetrical minibasins which later turn into minibasins with turtle structures (Figure 11b; e.g. Hudec et al., 2009; Peel, 2014). In the contraction domain, early contraction results in short wavelength folds and thrusts, which later develop into minibasins bounded by squeezed diapirs as the salt breaches the fold crests (Figure 11c; e.g. Fort et al., 2004; Rowan et al., 2004; Stewart & Coward, 1995). As the main control changes during upslope migration of the contractional domain, four more minibasin geometries are recognized based on their responses (Figure 11d and e). When the contractional domain migrates to the translational domain, early stage minibasins dominated by sediment loading become asymmetrical as the depocentre shifts away from the basin centre due to variations in the growth rate between the bounding diapirs (Figure 11d

early stage; Hudec et al., 2009). In contrast, when contraction migrates onto a mature minibasin with a strong turtle structure, deformation is localized on the adjacent salt diapirs which are uplifted forcing the flanking depocentres to migrate towards basin centre (Figure 11d late stage). When contraction migrates to the extensional domain, early stage extensional minibasins are inverted forming folds and thrusts (Figure 11e early stage). In contrast, when welded minibasins are compressed, the resultant minibasins tend to have a simple geometry defined by narrowed depocentres bounded by squeezed salt diapirs (Figure 11e late stage).

7 | CONCLUSIONS

Interpretation of three-dimensional seismic data from the Lower Congo Basin, calibrated with well data, enables analysis of the tectono-stratigraphic evolution of the supra-salt strata and assessment of various controls on minibasins and associated salt walls/pillows evolution.

Time-thickness maps and cross-sectional stratal geometries suggest that the present-day minibasin and salt wall configurations are the result of three main controls: thin-skinned extension, sediment loading and thin-skinned contraction. After a short initial period of tectonic quiescence, thin-skinned extension started from the Cenomanian to Coniacian and was characterized by a pervasive network of normal faults and rollovers. Subsequent minibasin and salt wall evolution was dominated by sediment loading and minibasin downbuilding, with a brief period of contraction affecting the southwest of the study area. Regional thin-skinned contraction occurred in the Miocene across the entire study area and resulted in squeezed salt walls and confined depocentres.

We show that minibasins develop from multiple initial depocentres that grow and merge over time as minibasins weld on the sub-salt. Moreover, as minibasins grow at different rates, variability of minibasin geometry associated with different stages of minibasin maturity exist between minibasins. Upslope migration of the contractional domain adds another layer of complexity and variability, because immature and mature minibasins respond to thin-skinned contraction differently.

Minibasin geometry and stratigraphic architecture show considerable variation related to the different kinematic domains during thin-skinned salt tectonics. Minibasins in the translational domain controlled by sediment loading tend to develop symmetrical geometries as they subside into the underlying salt and form turtle structure as they become welded. In contrast, minibasins in extensional and contractional domains have diagnostic extensional and contractional structures such as normal faults, and folds and thrusts, respectively. As contraction migrates upslope during thin-skinned salt deformation, sediment loading dominated minibasins are

superimposed by contraction and develop squeezed salt diapirs with shifted or confined depocentres. In contrast, extensionally driven minibasins tend to be inverted by contraction, developing folds and thrusts.


This study highlights the variability in 3D geometry, topography, stratigraphic architecture and evolution of minibasins. This variability in minibasin development contrasts with existing models which generally associate one minibasin with only one main control, namely extension, sediment loading or contraction depending on whether it formed in the extensional, translational or contractional domain during thin-skinned salt tectonics. Our results indicate that minibasin development is more complex, with factors such as along-strike coalescence of depocentres, variations in maturity, upslope migration of contraction, and multiple phases of thin-skinned deformation are important in their evolution.

ACKNOWLEDGEMENTS

We thank Equinor AS for sponsoring the Turbidites, Topography and Tectonics (T³) project and providing proprietary well data. ZG thanks financial support from Science Foundation of China University of Petroleum, Beijing (No. 2462020YXZZ020). We thank Sonangol, PGS and Equinor for providing access to seismic data and giving permission to publish the seismic sections in this paper. Schlumberger is thanked for providing Petrel software in the 3D Seismic Lab in the University of Bergen. We thank Chris Jackson and an anonymous reviewer for reviews that greatly improved the manuscript. The editor, Kerry Gallagher, is thanked for editing the paper. The authors have no conflict of interest to declare.

ORCID

Zhiyuan Ge  <https://orcid.org/0000-0002-6029-5512>

Rob L. Gawthorpe  <https://orcid.org/0000-0002-4352-6366>

REFERENCES

- Anderson, J. E., Cartwright, J., Drysdall, S. J., & Vivian, N. (2000). Controls on turbidite sand deposition during gravity-driven extension of a passive margin: Examples from Miocene sediments in Block 4, Angola. *Marine and Petroleum Geology*, *17*(10), 1165–1203. [https://doi.org/10.1016/S0264-8172\(00\)00059-3](https://doi.org/10.1016/S0264-8172(00)00059-3)
- Anka, Z., & Séranne, M. (2004). Reconnaissance study of the ancient Zaire (Congo) deep-sea fan. (ZaiAngo Project). *Marine Geology*, *209*(1), 223–244. <https://doi.org/10.1016/j.margeo.2004.06.007>
- Anka, Z., Seranne, M., Lopez, M., Scheck-Wenderoth, M., & Savoye, B. (2009). The long-term evolution of the Congo deep-sea fan: A basin-wide view of the interaction between a giant submarine fan and a mature passive margin (ZaiAngo project). *Tectonophysics*, *470*(1), 42–56. <https://doi.org/10.1016/j.tecto.2008.04.009>
- Banham, S. G., & Mountney, N. P. (2013). Evolution of fluvial systems in salt-walled mini-basins: A review and new insights. *Sedimentary Geology*, *296*, 142–166. <https://doi.org/10.1016/j.sedgeo.2013.08.010>
- Brice, S. E., Cochran, M. D., Pardo, G., & Edwards, A. D. (1982). Tectonics and Sedimentation of the South Atlantic Rift Sequence: Cabinda, Angola. In edited by J. S. Watkins and C. L. Drake. (Eds.) *Studies in Continental Margin Geology*. AAPG Memoir.
- Brun, J.-P., & Fort, X. (2004). Compressional salt tectonics (Angolan margin). *Tectonophysics*, *382*(3), 129–150. <https://doi.org/10.1016/j.tecto.2003.11.014>
- Brun, J.-P., & Fort, X. (2011). Salt tectonics at passive margins: Geology versus models. *Marine and Petroleum Geology*, *28*(6), 1123–1145. <https://doi.org/10.1016/j.marpetgeo.2011.03.004>
- Brun, J.-P., & Fort, X. (2012). Salt tectonics at passive margins: Geology versus models—Reply. *Marine and Petroleum Geology*, *37*(1), 195–208. <https://doi.org/10.1016/j.marpetgeo.2012.04.008>
- Callot, J.-P., Trocmé, V., Letouzey, J., Albouy, E., Jahani, S., & Sherhati, S. (2012). Pre-existing salt structures and the folding of the Zagros Mountains. *Geological Society, London, Special Publications*, *363*(1), 545–561. <https://doi.org/10.1144/SP363.27>
- Cramez, C., & Jackson, M. P. A. (2000). Superposed deformation straddling the continental-oceanic transition in deep-water Angola. *Marine and Petroleum Geology*, *17*(10), 1095–1109. [https://doi.org/10.1016/S0264-8172\(00\)00053-2](https://doi.org/10.1016/S0264-8172(00)00053-2)
- Dooley, T. P., Hudec, M. R., Pichel, L. M., & Jackson, M. P. (2018). The impact of base-salt relief on salt flow and suprasalt deformation patterns at the autochthonous, paraautochthonous and allochthonous level: Insights from physical models. *Geological Society, London, Special Publications*, *476*(SP476), 287–315.
- Duffy, O. B., Fernandez, N., Peel, F. J., Hudec, M. R., Dooley, T. P., & Jackson, C.-A.-L. (2019). Obstructed minibasins on a salt-detached slope: An example from above the Sigsbee canopy, northern Gulf of Mexico. *Basin Research*, *32*(3), 505–524. <https://doi.org/10.1111/bre.12380>
- Duval, B., Cramez, C., & Jackson, M. P. A. (1992). Raft tectonics in the Kwanza basin, Angola. *Marine and Petroleum Geology*, *9*(4), 389–404. [https://doi.org/10.1016/0264-8172\(92\)90050-O](https://doi.org/10.1016/0264-8172(92)90050-O)
- Evans, S. L., & Jackson, C. A. L. (2019). Base-salt relief controls salt-related deformation in the Outer Kwanza Basin, offshore Angola. *Basin Research*. <https://doi.org/10.1111/bre.12390>
- Fort, X., Brun, J.-P., & Chauvel, F. (2004). Salt tectonics on the Angolan margin, synsedimentary deformation processes. *AAPG Bulletin*, *88*(11), 1523–1544. <https://doi.org/10.1306/06010403012>
- Ge, Z., Gawthorpe, R. L., Rotevatn, A., Zijerveld, L., A.-L. Jackson, C., & Oluboyo, A., (2019). Minibasin depocentre migration during diachronous salt welding, offshore Angola. *Basin Research*. <https://doi.org/10.1111/bre.12404>
- Ge, Z., Rosenau, M., Warsitzka, M., & Gawthorpe, R. L. (2019). Overprinting translational domains in passive margin salt basins: Insights from analogue modelling. *Solid Earth*, *10*(4), 1283–1300. <https://doi.org/10.5194/se-10-1283-2019>
- Gemmer, L., Beaumont, C., & Ings, S. J. (2005). Dynamic modelling of passive margin salt tectonics: Effects of water loading, sediment properties and sedimentation patterns. *Basin Research*, *17*(3), 383–402. <https://doi.org/10.1111/j.1365-2117.2005.00274.x>
- Goteti, R., Ings, S. J., & Beaumont, C. (2012). Development of salt minibasins initiated by sedimentary topographic relief. *Earth and Planetary Science Letters*, *339–340*, 103–116. <https://doi.org/10.1016/j.epsl.2012.04.045>
- Hodgson, N. A., Farnsworth, J., & Fraser, A. J. (1992). Salt-related tectonics, sedimentation and hydrocarbon plays in the Central Graben, North Sea, UKCS. *Geological Society, London, Special Publications*, *67*(1), 31–63. <https://doi.org/10.1144/GSL.SP.1992.067.01.03>

- Hudec, M. R., & Jackson, M. P. A. (2007). Terra infirma: Understanding salt tectonics. *Earth-Science Reviews*, 82(1), 1–28. <https://doi.org/10.1016/j.earscirev.2007.01.001>
- Hudec, M. R., Jackson, M. P. A., & Schultz-Ela, D. D. (2009). The paradox of minibasin subsidence into salt: Clues to the evolution of crustal basins. *Geological Society of America Bulletin*, 121(1–2), 201–221.
- Ings, S. J., & Beaumont, C. (2010). Shortening viscous pressure ridges, a solution to the enigma of initiating salt ‘withdrawal’ minibasins. *Geology*, 38(4), 339–342. <https://doi.org/10.1130/G30520.1>
- Jackson, C.-A.-L., Rodriguez, C. R., Rotevatn, A., & Bell, R. E. (2014). Geological and geophysical expression of a primary salt weld: An example from the Santos Basin, Brazil. *Interpretation*, 2(4), SM77–SM89. <https://doi.org/10.1190/INT-2014-0066.1>
- Jackson, M. P. A., & Talbot, C. J. (1991). *A glossary of salt tectonics*. Austin: Bureau of Economic Geology, University of Texas.
- Jackson, M. P. A., Vendeville, B. C., & Schultz-Ela, D. D. (1994). Structural dynamics of salt systems. *Annual Review of Earth and Planetary Sciences*, 22, 93–117. <https://doi.org/10.1146/annurev.ev.22.050194.000521>
- Karner, G. D., Driscoll, N. W., McGinnis, J. P., Brumbaugh, W. D., & Cameron, N. R. (1997). Tectonic significance of syn-rift sediment packages across the Gabon-Cabinda continental margin. *Marine and Petroleum Geology*, 14(7–8), 973–1000. [https://doi.org/10.1016/S0264-8172\(97\)00040-8](https://doi.org/10.1016/S0264-8172(97)00040-8)
- Lavier, L. L., Steckler, M. S., & Brigaud, F. (2001). Climatic and tectonic control on the Cenozoic evolution of the West African margin. *Marine Geology*, 178(1), 63–80. [https://doi.org/10.1016/S0025-3227\(01\)00175-X](https://doi.org/10.1016/S0025-3227(01)00175-X)
- Lundin, E. R. (1992). Thin-skinned extensional tectonics on a salt detachment, northern Kwanza Basin. *Angola. Marine and Petroleum Geology*, 9(4), 405–411. [https://doi.org/10.1016/0264-8172\(92\)90051-F](https://doi.org/10.1016/0264-8172(92)90051-F)
- Marsh, N., Imber, J., Holdsworth, R., Brockbank, P., & Ringrose, P. (2010). The structural evolution of the Halten Terrace, offshore Mid-Norway: Extensional fault growth and strain localisation in a multi-layer brittle–ductile system. *Basin Research*, 22(2), 195–214. <https://doi.org/10.1111/j.1365-2117.2009.00404.x>
- Marton, G., Tari, G. C., & Lehmann, C. T. (2000). Evolution of the Angolan Passive Margin, West Africa, With Emphasis on Post-Salt Structural Styles. *Atlantic Rifts and Continental Margins*, 129–149.
- Mauduit, T., Gaullier, V., Brun, J. P., & Guerin, G. (1997). On the asymmetry of turtle-back growth anticlines. *Marine and Petroleum Geology*, 14(7), 763–771. [https://doi.org/10.1016/S0264-8172\(97\)00053-6](https://doi.org/10.1016/S0264-8172(97)00053-6)
- Moulin, M., Aslanian, D., Olivet, J.-L., Contrucci, I., Matias, L., Géli, L., ... Unternehr, P. (2005). Geological constraints on the evolution of the Angolan margin based on reflection and refraction seismic data (ZaiAngo project). *Geophysical Journal International*, 162(3), 793–810. <https://doi.org/10.1111/j.1365-246X.2005.02668.x>
- Nürnberg, D., & Müller, R. D. (1991). The tectonic evolution of the South Atlantic from Late Jurassic to present. *Tectonophysics*, 191(1), 27–53. [https://doi.org/10.1016/0040-1951\(91\)90231-G](https://doi.org/10.1016/0040-1951(91)90231-G)
- Oluboyo, A. P., Gawthorpe, R. L., Bakke, K., & Hadler-Jacobsen, F. (2014). Salt tectonic controls on deep-water turbidite depositional systems: Miocene, southwestern Lower Congo Basin, offshore Angola. *Basin Research*, 26(4), 597–620. <https://doi.org/10.1111/bre.12051>
- Peel, F. J. (2014). How do salt withdrawal minibasins form? Insights from forward modelling, and implications for hydrocarbon migration. *Tectonophysics*, 630, 222–235. <https://doi.org/10.1016/j.tecto.2014.05.027>
- Rowan, M. G., Peel, F. J., & Vendeville, B. C. (2004). Gravity-driven fold belts on passive margins. In K. R. McClay (Ed.), *Thrust tectonics and hydrocarbon systems*, Vol. 82 (pp. 157–182). AAPG Memoir.
- Rowan, M. G., & Vendeville, B. C. (2006). Foldbelts with early salt withdrawal and diapirism: Physical model and examples from the northern Gulf of Mexico and the Flinders Ranges. *Australia. Marine and Petroleum Geology*, 23(9), 871–891. <https://doi.org/10.1016/j.marpetgeo.2006.08.003>
- Rowan, M. G., & Weimer, P. (1998). Salt-sediment interaction, northern Green Canyon and Ewing bank (offshore Louisiana), northern Gulf of Mexico. *AAPG Bulletin*, 82(5), 1055–1082.
- Stewart, S. A., & Coward, M. P. (1995). Synthesis of salt tectonics in the southern North Sea. *UK. Marine and Petroleum Geology*, 12(5), 457–475. [https://doi.org/10.1016/0264-8172\(95\)91502-G](https://doi.org/10.1016/0264-8172(95)91502-G)
- Valle, P. J., Gjelberg, J. G., & Helland-Hansen, W. (2001). Tectonostratigraphic development in the eastern Lower Congo Basin, offshore Angola, west Africa. *Marine and Petroleum Geology*, 18(8), 909–927. [https://doi.org/10.1016/S0264-8172\(01\)00036-8](https://doi.org/10.1016/S0264-8172(01)00036-8)
- Vendeville, B. C., & Jackson, M. P. A. (1992). The rise of diapirs during thin-skinned extension. *Marine and Petroleum Geology*, 9(4), 331–354. [https://doi.org/10.1016/0264-8172\(92\)90047-I](https://doi.org/10.1016/0264-8172(92)90047-I)
- Wagner, B. H., & Jackson, M. P. (2011). Viscous flow during salt welding. *Tectonophysics*, 510(3), 309–326. <https://doi.org/10.1016/j.tecto.2011.07.012>

How to cite this article: Ge Z, Gawthorpe RL, Zijerveld L, Oluboyo AP. Spatial and temporal variations in minibasin geometry and evolution in salt tectonic provinces: Lower Congo Basin, offshore Angola. *Basin Res.* 2020;00:1–18. <https://doi.org/10.1111/bre.12486>